Turkish Journal of Electrical Engineering & Computer Sciences

http://journals.tubitak.gov.tr/elektrik/

Research Article

Turk J Elec Eng & Comp Sci
(2016) 24: 793 – 806
© TÜBİTAK
doi:10.3906/elk-1306-206

Sizing design and implementation of a flywheel energy storage system for space applications

Kutlay AYDIN[1,*], **Mehmet Timur AYDEMİR**[2]
[1]Turkish Aerospace Industries, Inc., Kazan, Ankara, Turkey
[2]Department of Electrical and Electronic Engineering, Faculty of Engineering, Gazi University, Ankara, Turkey

Received: 23.06.2013 • **Accepted/Published Online:** 01.10.2013 • **Final Version:** 23.03.2016

Abstract: Flywheel energy storage systems have become an important research subject in recent years. They are also considered for space applications instead of hazardous and bulky electrochemical batteries. In this paper, a flywheel energy storage system has been designed for satellite attitude control systems. Power requirements of a small commercial satellite have been used as the starting point of the design. The designed system includes a BLDC motor. The machine is run as a motor for 60 min and the stored energy is discharged during the following 30 min to simulate low orbit satellite operation. Experimental results show that these systems can be used in space applications.

Key words: Flywheel energy storage, motor-generator operation, satellite attitude control systems

1. Introduction

Flywheels are devices that store kinetic energy on their rotating masses. These devices are considered to be among the alternatives of electrochemical batteries. Electrochemical batteries are known to have some disadvantages that affect their usage in space applications. The most important drawbacks of electrochemical batteries are the impossibility of replacement of batteries on board and the low number of their charge-discharge cycles. These also affect the mission and, therefore, batteries are very critical components of space applications. As a result of these disadvantages and the advancements in electronics, materials, and mechanics, strong interest has been directed towards flywheel energy storage. However, the most promising idea is to integrate the flywheels and attitude control systems of satellites, since it also leads to a dramatic gain in volume and weight [1,2].

Flywheel systems have been under research at NASA's Glenn Research Center. It is reported that in order to attain desired features such as long life, high efficiency, and low sensitivity to temperature changes high-strength composite wheels and magnetic suspension need to be considered [3].

The design, implementation, and experimental results of a flywheel energy storage system that can be used in satellite attitude control system are presented in this paper. The design has been carried out according to the power requirements of a real satellite subsystem. Battery charge and discharge periods have been determined depending on the orbit and power system requirements. A controller has also been designed for the system. The controller design has been made such that it acts properly to compensate the effects of system losses. Bus voltage regulation during the discharge period is also handled by energy storage and control units. Bus voltage regulation was successfully attained even at high and variable frequency operation due to a simple synchronization technique that was applied during the discharge interval [1].

*Correspondence: kaydin@tai.com.tr

In flywheel sizing a maximum amount of energy storage is aimed at within the technical limits of the material and equipment chosen. Mechanical strength of the material, maximum speed of the motor/generator, system losses, and physical dimensions are the most important design parameters [4–6].

In [7] voltage regulation of a space station was achieved by using an energy storage gyroscope. The power coming from the solar panels feed the load and the gyroscope during the period where the satellite sees the sun. This is called the "charging phase" of the gyroscope. In the charging mode the motor accelerates, reaches the rated speed, and continues to rotate at this speed. The kinetic energy stored in the gyroscope in this mode is converted back to electrical energy to supply the load in the period called the "discharge period", during which solar energy is not available for the satellite. In this mode the line voltage regulation is also achieved by the gyroscope. Between the charging and discharging periods there is a transition period called "charge reduction", in which solar energy is at a low level and only a small amount of energy can be received from solar panels. In this mode the gyroscope is also in charge of line voltage regulation.

The motor/generator unit is the most critical component of flywheel energy storage systems. Therefore, its selection and control design need to be carried out first. Typically, permanent magnet AC synchronous motors are the primary choice in applications due to their high efficiency and brushless structure. In the literature sensorless techniques have been suggested to reduce the hardware requirements and get rid of the limitations imposed by sensors [8–10]. Although there are several research projects about these techniques, the technique is not mature enough to use in space applications.

Because of their high performance and low cost, brushless DC motors can also be used in flywheel energy storage devices that are widely used in continuous energy systems [11].

A high-speed flywheel design and analyses of the losses of a flywheel were presented in [12]. Magnetic bearing was proposed to reduce the mechanical losses and it was reported that windage losses can be neglected if vacuum housing is used. The efficiency of the flywheel at the maximum speed was given as 95.98% but the energy efficiency (round-trip efficiency) was not given.

A low-speed micro flywheel energy storage system was designed in [13]. Passive magnetic bearing was proposed to levitate the rotor without any mechanical contact with the stator. It was reported that, to achieve high efficiency, the system was operated under a vacuum environment. However, the system efficiency was not given in this paper either.

A review of flywheel-based energy storage systems was presented in [14]. All the components (motor, bearing, housing, wheel, power converter) of a flywheel were evaluated. In order to reduce losses, magnetic bearing and vacuum housing must be used. Under vacuum conditions (neglecting windage losses) and without mechanical losses (by using magnetic bearing), the flywheel efficiency was given at around 90%–95%.

In this paper sizing of a flywheel energy storage unit is aimed. First, parametric equations to be used in the design are derived from the energy balance of the system. Then component selection is made, and parameters that affect the energy balance are determined. Finally, system sizing is carried out using these parameters.

The sizing design of the system is presented in Section 2. Motor-generator selection is given in Section 3. Experimental results are discussed in Section 4.

2. Sizing of flywheel energy storage device

Before starting a detailed system design, the design requirements need to be defined.

The duty of the storage device is to provide the required energy to satellite subsystems during the dark

period in orbit. In this paper, the power requirement of the S-band transmitter of the BilSat satellite is used as the starting point of the design. This piece of equipment consumes 23 W during data transfer [15]. Since the dark period is approximately 30 min for low earth orbit satellites, the energy consumption for this device is calculated to be 11.5 Wh for the worst case, assuming that the transfer is continuous.

2.1. Energy balance of the system

The design should have an iterative process and all the parameters are dependent on each other. The starting point of the design is the value of the kinetic energy stored in the wheel of the motor/generator unit while it is rotating at the maximum speed. This value is given in Eq. (1).

$$E_{tot} = \frac{1}{2} J \omega_{\max}^2 \tag{1}$$

The main function of the flywheel in the application is attitude control and therefore its speed needs to be above a minimum for all operating conditions such that the minimum momentum value is attained. Flywheel speed can be varied between this minimum speed and maximum speed. The difference between the energy amounts at these two speeds is the energy that can be usable by the system. This difference is defined as the depth of discharge (DD).

$$E_{diff} = \frac{1}{2} J \left(\omega_{\max}^2 - \omega_{\min}^2\right) \tag{2}$$

Eq. (1) is valid for a lossless system. The effective energy amount can also be found by incorporating the round-trip efficiency (η) in the equations.

$$E_{eff} = \eta \frac{1}{2} J \left(\omega_{\max}^2 - \omega_{\min}^2\right) = \eta\, E_{diff} \tag{3}$$

The round-trip efficiency used in Eq. (3) is defined to be the ratio of the energy recovered during the generator operation to the energy supplied during the motor (storing) operation. Round-trip efficiency value varies depending on the operation speed intervals.

Since the instantaneous efficiency will be varying for variable load and operation conditions, the speed interval needs to be determined first. The basic equation to start the process is the electromechanical torque equation. During the motor operation:

$$T_{em} = J \frac{d\omega}{dt} + B\,\omega + T_L \tag{4}$$

The torque equation during the discharge (generator) interval is given as follows:

$$J \frac{d\omega}{dt} = T_{em} + T_L + B\omega \tag{5}$$

As is obvious in this equation, energy flow is reversed, and the source now is the stored energy. It should also be noted that the windage losses are not omitted here since the experimental set-up will still have them, although they are expected to be zero in a real space application. The load torque, on the other hand, is zero since there is not such a load in the system.

The system round-trip efficiency between any two time instants can be rewritten as follows by using the fact that energy is the time-integral of power, and power is equal to torque times the speed.

$$\eta = \frac{E_e}{E_{diff}} = \frac{\int_{t1}^{t2} T_{em}\omega \, dt}{\frac{1}{2}J(\omega_{\max}^2 - \omega_{\min}^2)} \tag{6}$$

Friction losses in the flywheel systems can be reduced by using either magnetic bearings or oilless bearings. Although there is no load to oppose in the system, windage losses in systems without sufficient vacuum levels and disturbance torques for various reasons still exist.

2.2. System design

Precision ball bearings have been used in the designed system and all the requirements will be determined based on this. As a result of this choice, mechanical friction losses need to be considered in the design.

As there are many unknowns, it is required that some of the parameter values are chosen and the rest are calculated. The inertia of the flywheel has been taken as 0.008 kgm^2. The weight of the system now depends on this value as well as the material selection and mechanical design. Aluminum material has been used as the material to build the flywheel. Eventually, a disk-shaped flywheel of 20 cm in diameter and 2 kg in weight was obtained. Figure 1 shows the solid work of the flywheel design.

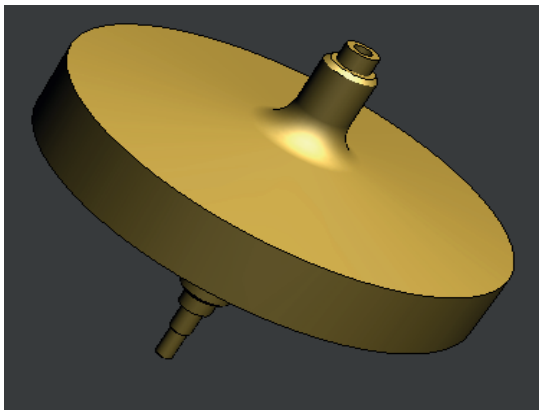

Figure 1. Solid work of the flywheel design.

As stated earlier, a minimum value of the angular momentum exists for the attitude control system. This value is $\mathrm{H}_{min} = 0.4$ Nms for the satellite used in the design. Minimum speed of the operation is obtained now by using these values.

$$H_{\min} \leq J\,\omega_{\min} \;\Rightarrow \omega_{\min} \geq (0.4\ Nms)/(0.008\ kg.m^2) = 50\ rad/s = 477.46\ RPM$$

Although this value will guarantee the operation of the attitude system, the voltage generated at this speed by the flywheel will be very small to regulate the bus. Therefore, the value for the minimum speed was chosen to be 5000 rpm. On the other hand, the minimum speed is not chosen bigger than 5000 rpm to keep the depth of discharge as big as possible.

It is not proper to define a specific efficiency for the generator due to variable speed operation. Therefore, it would be a better approach to use the energy balance equation (Eq. (7)) to determine the operation speed

interval.

$$\begin{aligned} \tfrac{1}{2}J(\omega_{\max}^2 - \omega_{\min}^2) &= \int_{t1}^{t2} T_{em}\omega dt + \int_{t1}^{t2} B\omega^2 dt \\ &= \int_{t1}^{t2} T_{em}\omega dt + \int_{t1}^{t2} P_{fr} dt + \int_{t1}^{t2} P_{wind} dt \end{aligned} \tag{7}$$

Speed variation in the generator mode of operation is linear only if the load is constant. However, the load is never constant because of the speed-dependent losses. This is especially true for the ground prototype due to the windage losses. On the other hand, assuming a constant load simplifies the design. A multiplier is introduced in the controller to compensate this error.

2.2.1. Calculation of the electrical machine losses

The first term on the right side of Eq. (7) represents the net energy consumed for electrical load and electrical losses. The energy required by the load has already been determined to be 11.5 Wh (41,400 J). The efficiency of the machine used (details of which are given in the Appendix) is 93% and load power is assumed to be constant at 23 W. This means that the electrical losses are approximately 1.73 W and this corresponds to an energy loss of 0.865 Wh.

2.2.2. Calculation of the mechanical friction losses

The second term in the right side of Eq. (7) shows the mechanical friction losses. Total losses for the two bearings used in the wheel are given as [16]:

$$P_{fr} = 2\left[f_v(\nu\frac{30}{\pi}\omega)^{2/3}D_b^3\,10^{-10}\omega\right] + 2\left[\omega\, f_L\, F\, D_b\right] \tag{8}$$

The first term in Eq. (8) is the friction losses due to the viscosity of the liquid used in the bearings. The second term is the mechanical friction losses, which depend on the forces acting on the bearings.

The calculations based on the technical specifications of some well-known commercial bearings yielded that the first term reaches very high values for the conditions under consideration so that the mission becomes impossible. Therefore, bearings of oilless type have been chosen for the application. As a result, the first term in the equation can be dropped.

In order to calculate the losses due to the bearing friction, the forces acting on the bearings need to be known. In this system these forces are the force due to the wheel weight (F_G) and forces due to unbalances (F_B). Thus, the total force is given as:

$$F = F_G + FB \tag{9}$$

Unbalance force is defined as:

$$F_B = me\omega^2 \tag{10}$$

As a result, the total force equation becomes:

$$F = F_G + F_B = Mg + me\omega^2$$

If this equation is inserted into Eq. (8), the following power loss components are obtained:

$$\begin{aligned} P_G &= \omega f_L D_b F_G = \omega f_L D_b \left(\tfrac{M}{2}g\right) \\ P_B &= \omega f_L D_b F_B = \omega f_L D_b (me\omega^2) \end{aligned} \tag{11}$$

2.2.3. Calculation of windage losses

Since an attitude control system is supposed to work under vacuum in space, the windage losses are expected to be zero. However, the system designed here cannot be tested in similar conditions and it is inevitable that there will be some losses, and these losses should be accounted for in the design.

For the disk-shaped flywheels windage losses are defined as follows [17]:

$$P_{wind} = \frac{1}{64} C_M \rho \omega^3 D_r^5 \tag{12}$$

In order to calculate the torque coefficient in the equation first the Reynolds number needs to be found:

$$F = F_G + FB \tag{13}$$

In the experimental set-up a level of 5 mbar was achieved. The value of m is 1.93 $\times$ 10^{-5} kg/m s at 40 °C. The air density at this temperature and 5 mbar pressure is 0.0056 kg/m^3. Therefore, for a flywheel with 20 cm diameter, the torque coefficient is found to be [17]:

$$C_M = \frac{3.870}{R_e^{0.5}} \tag{14}$$

The windage loss equation now can be reorganized as follows now:

$$\begin{array}{l} P_{wind} = \frac{1}{64} \frac{2\,(3.870)\,\sqrt{\mu}}{D_r \sqrt{\rho\,\omega}} \rho\,\omega^3\,D_r^5 = \\ (0.121)\,(D_r^4 \sqrt{\mu\,\rho}\,\omega^{2.5}) \end{array} \tag{15}$$

Eq. (7) can be written as follows by taking the electrical energy amount to be 12.64 Wh (including electrical losses):

$$\frac{1}{2} J(\omega_{\max}^2 - \omega_{\min}^2) = (12.55)\,(3600) + \int_{t1}^{t2} P_G\,dt + \int_{t1}^{t2} P_B\,dt + \int_{t1}^{t2} P_{wind}\,dt \tag{16}$$

Speed variation is assumed to be linear in the design. As a result, the variation of angular speed can be defined with [ω_{max} – ($\Delta\omega$ / Δt) $\times$ t]. Now the energy balance equation can be rewritten. This assumption of linearity will of course introduce some errors in the results, and the losses will be higher than they actually are. Therefore, a coefficient of 0.542 is used to correct the error. This coefficient is calculated from the area ratios shown in Figure 2, the area under the discharge curve with constant load conditions and the area under the discharge curve with the load condition that is proportional to the 2.5th power of the speed (windage losses).

$$\begin{array}{rcl} \frac{1}{2} J(\omega_{\max}^2 - \omega_{\min}^2) & = & (12.55)\,(3600) \\ & & +2\,(0.542) \int_{t1}^{t2} f_L\,D_b(\frac{M}{2} g)\,[\omega_{\max} - (\Delta\omega/\Delta t)t]\,dt \\ & & +2\,(0.542) \int_{t1}^{t2} f_L\,D_b(me)\,[\omega_{\max} - (\Delta\omega/\Delta t)t]^3\,dt \\ & & +0.542 \int_{t1}^{t2} (0.121)\,D_r^4 \sqrt{\mu\rho}\,[\omega_{\max} - (\Delta\omega/\Delta t)t]^{2.5}\,dt \end{array} \tag{17}$$

If these integrations are carried out from t1 = 0 to a specific time, say t2 = T, the following result is obtained.

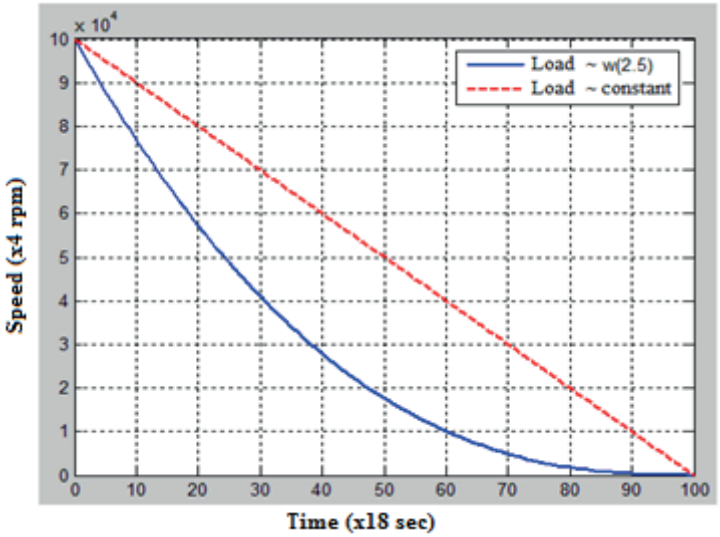

Figure 2. Speed–time graphics for different load profiles.

$$\begin{aligned}\tfrac{1}{2}J(\omega_{\max}^2-\omega_{\min}^2) &= (12.55)(3600)\\ &+(0.542)\,f_L\,D_b(Mg)\tfrac{T(\omega_{\max}^2-\omega_{\min}^2)}{2(\omega_{\max}-\omega_{\min})}\\ &+(2)(0.542)\,f_L\,D_b(me)\,\tfrac{T(\omega_{\max}^4-\omega_{\min}^4)}{4(\omega_{\max}-\omega_{\min})}\\ &+(0.542)(0.121)\,D_r^4\sqrt{\mu\rho}\,\tfrac{T\,(\omega_{\max}^{3.5}-\omega_{\min}^{3.5})}{3.5(\omega_{\max}-\omega_{\min})}\end{aligned} \tag{18}$$

The design parameters are given in the Table. Multiplication of the residual mass and its distance (m × e) is given for the unbalance. This value is obtained from the experimental work for balancing. Bearing parameters belong to the low-friction FAG bearings [18].

Table. Design parameters.

Parameter	Value
f_L	0.00028
D_b	(15 + 32) / 2 = 23.5 mm
m*e	5 g mm
T	1800 s (30 min)
J	0.008 kgm^2
ω_{min}	5000 rpm
M	2 kg
g	9.8 m/s^2
D_r	0.2 m
μ	1.93e-5 kg/m s
ρ	0.0056 kg/m^3

The only unknown in Eq. (18) is the maximum speed. By solving the equation its value is found to be 4243 rad/s (∼40,500 rpm). Depth of discharge (DD) can be obtained from this speed value now.

$$DD = 1-\frac{\omega_{\min}}{\omega_{\max}} = 1-\frac{523.6}{4243} \approx 87.7\% \tag{19}$$

By placing the maximum and minimum speed values in Eq. (2) the energy difference is found as 19.7 Wh, of which only 11.5 Wh is converted to electrical energy. As a result, the round-trip efficiency under these conditions is:

$$\eta = \frac{E_e}{E_{diff}} 100\% = \frac{11.5}{19.7} 100\% \approx \ 58.4\% \tag{20}$$

Mechanical friction and winding losses can be found from Eq. (18).

$$E_{fr} + E_{wind} = 7.06\ Wh \tag{21}$$

The maximum instantaneous value of torque that should be generated during motor operation can be found from Eq. (4). This value is attained when the friction is the highest, i.e. at the maximum speed.

$$\begin{aligned} &T_{em} = T_{acc} + T_{fr} + T_{wind} \\ &T_{acc} = J \tfrac{d\omega}{dt} \\ &T_{fr} = (2) f_L\, D_b \tfrac{M}{2} g + (2)\, f_L\, D_b (m\, e\, \omega_{\max}^2) \\ &T_{wind} = (0.121)\, D_r^4 \sqrt{\mu \rho}\, \omega_{\max}^{1.5} \end{aligned} \tag{22}$$

The motor mode lasts 60 min and the speed is linearly increased in this mode from the minimum to the maximum value. Therefore, the speed difference is 40,500 – 5000 = 35,500 rpm. Thus:

$$\begin{aligned} &T_{acc} = 8.26 mNm \\ &T_{fr} = 1.31 mNm (\max) \\ &T_{wind} = 17.53 mNm (\max) \\ &\Rightarrow T_{em} = 27.10 mNm \end{aligned} \tag{23}$$

If the design is carried out for the space environment, by taking the windage losses as zero, maximum speed is found to be 3450 rad/s (32,900 rpm). This yields a difference in energy of 12.92 Wh, of which 11.5 Wh is converted to electrical energy, and a round-trip efficiency of 89%.

If the torque component corresponding to windage losses is subtracted in Eq. (22), the maximum torque that the machine needs to generate ($T_{em} = T_{acc} + T_{fr}$) is found as 9.34 mNm. This shows that the highest component is the windage torque, and if it does not exist, efficiency increases and a smaller motor would be sufficient for the application.

3. Determining the type of the electric machine

The selection process of the electrical machine for the application is described in this section. Three types of machines are evaluated for this application: DC machines, induction machines, and synchronous machines.

Brush-type DC machines cannot be considered since their brushes prevent them from high-speed applications. Brushes also reduce the lifetime of the machines and need maintenance, which make them unsuitable for space applications.

Induction machines are brushless, cheap, and simple. Therefore, they are preferred for mechanical batteries in ground applications. However, it is difficult to maintain electrodynamic stability in variable operation conditions [2]. Also, the rotor copper losses are very high, especially at high slip values. Therefore, these machines are also eliminated from the list of choices.

Synchronous machines can be divided into subgroups: field excited synchronous machines, permanent magnet synchronous (PMAC) machines, brushless DC (BLDC) machines, and synchronous reluctance machines.

Energy flows in both directions in flywheel applications. Although there are generator applications of permanent magnet reluctance machines, difficulties in the parameter measurement and estimation complicate the controllers. They also suffer from cogging torques [19–21]. Therefore, these machines are eliminated from the list, too. The field excited synchronous machines are also eliminated for the same reasons as the brush-type DC machines.

PMAC machines have magnets on their rotors and therefore do not need brushes. As there are no windings on the rotor, total copper losses are reduced. These machines therefore are suitable for mechanical battery applications.

BLDC machines are similar to PMAC machines except for their winding and magnet placements. As a result, the back emf waveform is trapezoidal in BLDC machines whereas it is sinusoidal in PMAC machines. The driving method of these machines is simpler and the high torque per ampere feature makes them the best candidate for this application.

In the application a BLDC motor of Maxon (EC25) has been chosen. Its technical specifications are given in the Appendix. This is a 36 V machine with 6100 rpm maximum speed. A Maxon driver (DEC 70/10) was also used to drive the motor. The current reference was derived from the desired speed profile and transferred to this driver through a computer.

4. Experimental work

A prototype of the machine was built and tested. The solid model of the flywheel and the prototype are shown in Figure 3. The wheel is placed on ball bearings on both sides. A high-speed flexible coupling was used for the motor–flywheel connection.

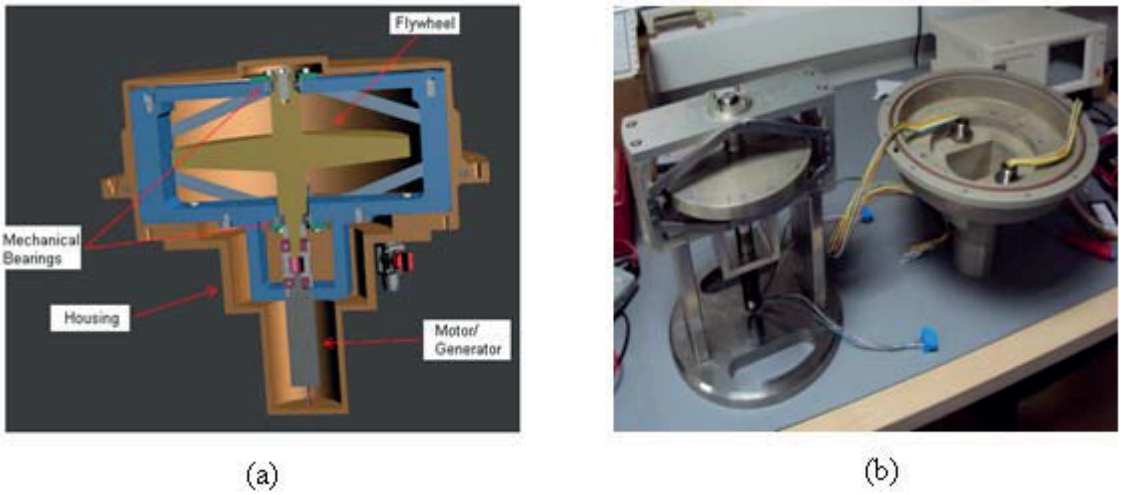

Figure 3. a) Solid model of the flywheel, b) prototype.

A functional diagram of the test bed is seen in Figure 4. The switch in the figure removes the supply connections and connects the terminals of the machine to a three-phase load. The energy measurements are carried out directly at the generator outputs.

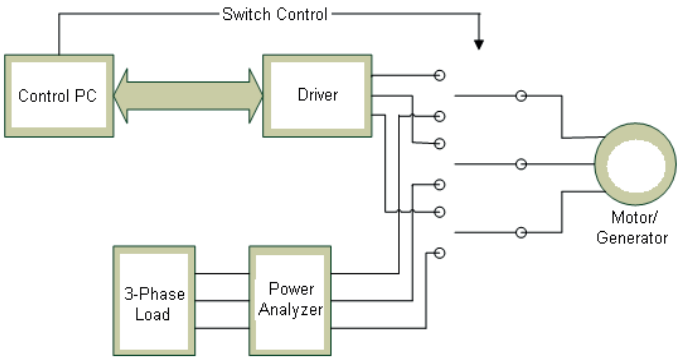

Figure 4. Functional block diagram of the experimental set-up.

The motor/generator and flywheel set was vacuumed down to 5 mbar for the experiments. The motor was driven for approximately 10 min at constant current to reach 5000 rpm. After this speed, the current reference was modified to compensate the effects of losses for 60 min. An operation loop lasts for 1000 min : 60 min in motor mode and 30 min in generator mode. Speed variation obtained in a complete loop is given in Figure 5. Flywheel speed is limited to 39,600 rpm due to the technical specifications of the driver.

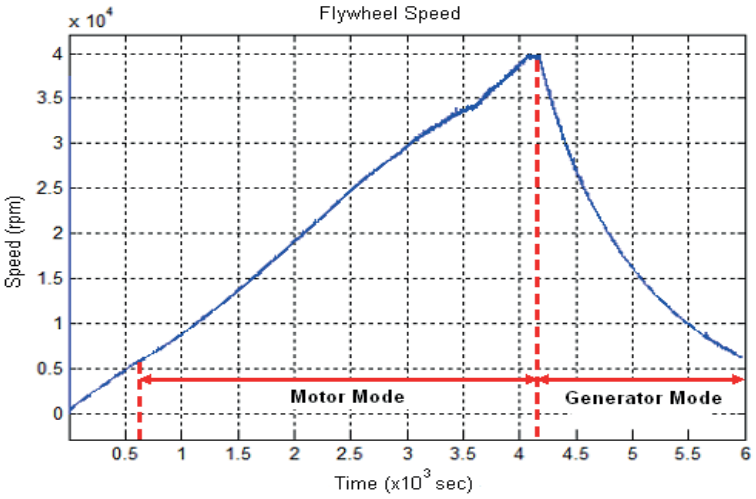

Figure 5. Speed variation for a complete loop of operation,

Mechanical resonances were observed in the system caused by the mechanical design and bearings of the system. The most dominant one was seen between 30,000 and 35,000 rpm. However, the controller was able to overcome the disturbances and the speed profile was followed. Figure 6 shows the speed profile and the actual speed in the motor mode of operation.

Figure 7 shows the variation of the current reference obtained from the speed error. If the speed is below the reference the current reference increases to catch up. This is especially obvious in the mechanical resonance region.

The load during the discharge (generator) mode was a three-phase load with 2.7 Ω per phase connected in star. The speed variation in this mode is given in Figure 5. This mode lasts for 30 min and 11 Wh net energy was measured at the output of the generator. This corresponds to a round-trip efficiency of 58.9%, which is higher than estimated.

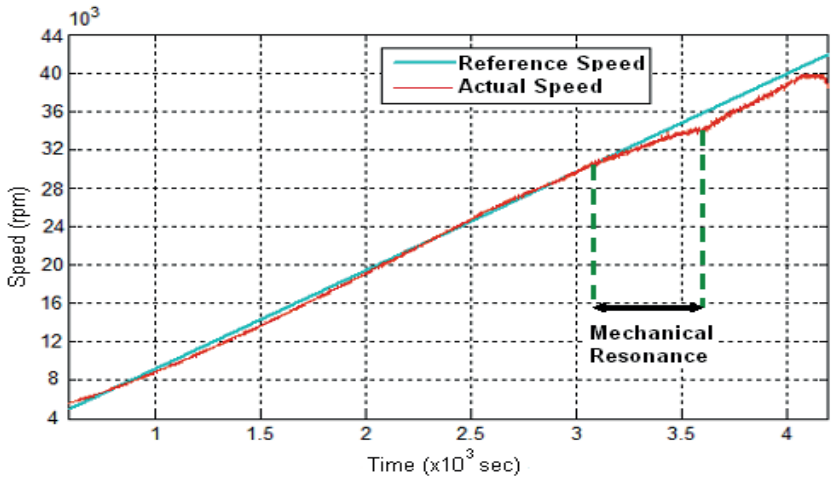

Figure 6. Speed reference and actual speed variation during motor mode.

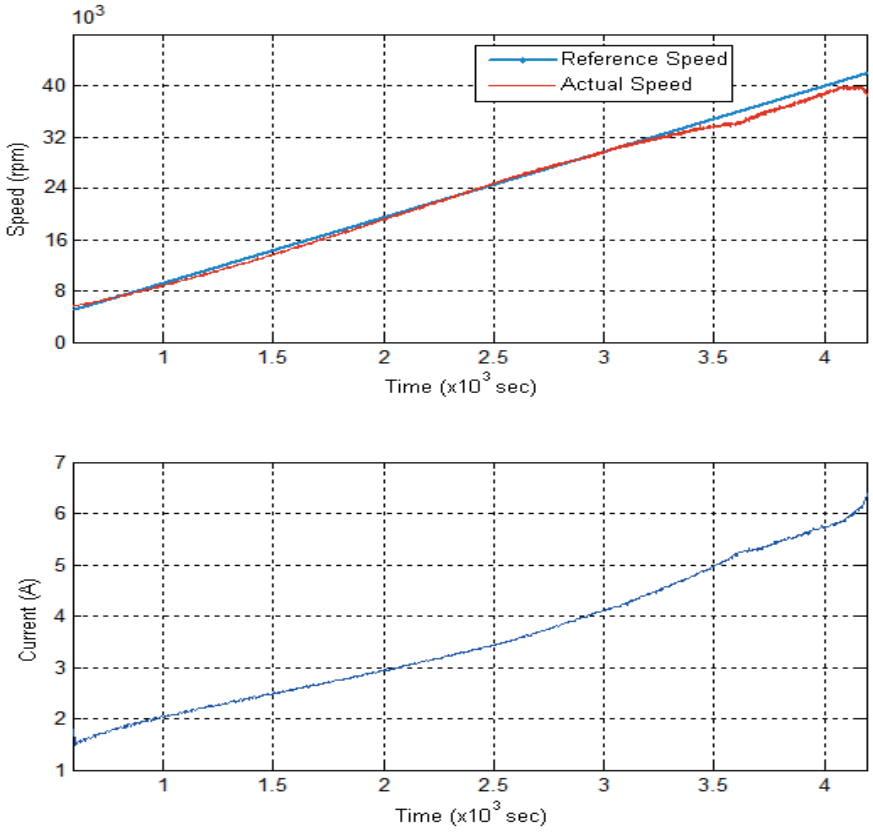

Figure 7. Adjustment of the current reference as a function of the speed error.

Figure 8 shows the energy recovery during the generator mode along with the speed variation.

Experimental results show that the system design was successful. There are some small mismatches, especially due to mechanical resonance, but the overall aim was reached.

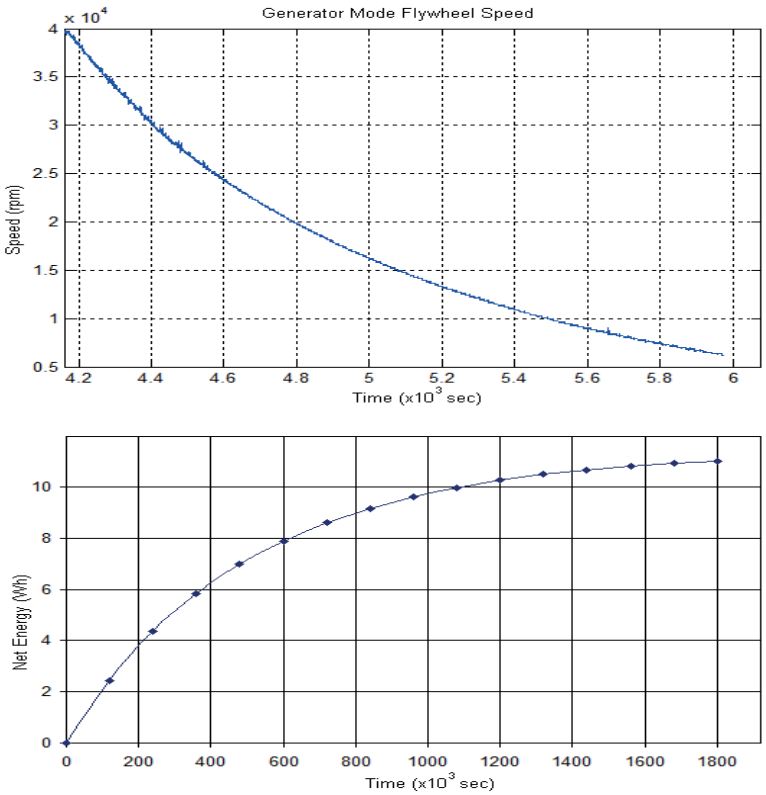

Figure 8. Speed and recovered net energy during generator mode.

5. Conclusion

Flywheels are among the devices that are used to store energy to be used later. They are supposed to have large inertia values and when operated at high speeds they can store large amounts of energy. A good quality flywheel energy system is required to have very low bearing losses to be efficient.

Recently there has been an interest in using them in aerospace applications both to store energy and to control the attitude of satellites. In this paper, sizing and implementation of a high-speed flywheel energy storage system aimed for aerospace applications was reported. System sizing was done by using system energy balance equations. After the equipment and material selection, production and system integration were achieved. The results of the experimental study show that real and calculated parameters are in good agreement.

High windage losses of the system are an important issue for these systems and they increase as the size of the flywheel surface area increases. The system should be operated in hard vacuum conditions to keep the windage losses at a near-zero level. However, hard vacuum condition was not possible to attain in this work because of the available low performance infrastructure. As a result, the windage losses could not be eliminated. Theoretical calculations yielded that a round-trip efficiency of 58.4% could be expected for the designed system under earth conditions. The round-trip efficiency obtained in the experimental work was slightly higher at 58.9%. Theoretical calculations show that the expected round-trip energy efficiency of the designed system in a spacecraft (in a vacuum environment) is 89%.

Mechanical losses and size are two important factors when a flywheel energy storage system is designed for aerospace applications. To achieve high energy efficiencies in these systems magnetic suspension and integrated motor/wheel-based designs are planned for future work.

Nomenclature

B	Viscous friction coefficient (Nms)
E_{diff}	Energy that can be recovered from the wheel (J)
C_M	Torque constant
D_b, D_i, D_o	Average, inner, and outer diameters of bearing (mm)
D_r	Wheel diameter (m)
e	Eccentricity between the gravity center and axis of rotation of the wheel (m)
E_{max}	Maximum value of the energy stored in the wheel (J)
F	Total force acting on bed (N)
f_v	Speed-dependent friction coefficient
g	Gravity ($\sim$9.8 m/s^2)
H	Angular momentum (Nms)
J	Total moment of inertia of the rotor and wheel (kgm^2)
f_L	Load-dependent friction coefficient
M	Mass of the wheel (kg)
m	Residual mass (kg)
ω	Dynamic viscosity of air (kg/m s)
ω	Wheel speed (rad/s)
ω_{min}	Minimum speed of the wheel (rad/s)
ω_{max}	Maximum speed of the wheel (rad/s)
P_B	Friction power due to unbalance forces (W)
P_G	Friction power due to gravity (W)
ρ	Air density (kg/m^3)
T_{acc}	Acceleration torque (Nm)
T_{em}	Electromechanic torque (Nm)
T_L	Load torque (Nm)
v	Kinematical viscosity of bearing liquid (mm^2/s)

References

[1] Kenny BH, Kascak PE, Jansen R, Dever TP, Santiago, W. Control of a high-speed flywheel system for energy storage in space applications. IEEE T Ind Appl 2005; 41: 1029-1038.

[2] Patel MR. Spacecraft Power Systems. New York, NY, USA: CRC Press, 2005.

[3] Lyons VJ. Aerospace power technology for potential terrestrial applications. In: Energytech; 2012; Cleveland, OH, USA. pp. 1-5.

[4] Tsao P, Senesky M, Sanders SR. An integrated flywheel energy storage system with homopolar inductor motor/generator and high-frequency drive. IEEE T Ind Appl 2003, 39: 1710-1725.

[5] Siostrzonek T, Penczek A, Pirog S. The control and structure of the power electronic system supplying the flywheel energy storage (FES). In: European Conference on Power Electronics and Applications; 2007; Aalborg, Denmark. pp. 1-8.

[6] Beaman BG, Rao GM. Hybrid battery and flywheel energy storage system for LEO spacecraft. In: Battery Conference on Applications and Advances; 1998; Long Beach, CA, USA. pp. 113-116.

[7] Kascak PE, Kenny BH, Dever TP, Santiago W, Jansen RH. International Space Station Bus Regulation with NASA GRC Flywheel Energy Storage System Development Unit. NASA/TM-2001-211138. Cleveland, OH, USA: NASA, 2001.

[8] Kenny BH, Kascak PE, Hofmann H, Mackin M, Santiago W, Jansen R. Advanced Motor Control Test Facility for NASA GRC Flywheel Energy Storage System Technology Development Unit. NASA/TM-2001-210986. Cleveland, OH, USA; NASA, 2001.

[9] Kenny BH, Kascak PE. Sensorless Control of Permanent Magnet Machine for NASA Flywheel Technology Development. NASA/TM-2002-211726. Cleveland, OH, USA; NASA, 2002.

[10] Kenny BH, Santiago W. Filtering and Control of High Speed Motor Current in a Flywheel Energy Storage System. NASA/TM-2004-213343. Cleveland, OH, USA; NASA, 2004.

[11] Junling C, Xinjian J, Dongqi Z, Haigang W. A novel uninterruptible power supply using flywheel energy storage unit. In: The 4th International Power Electronics and Motion Control Conference; 2004; Xi'an, China. pp. 1180-1184.

[12] Zhang C, Tseng KJ, Nguyen TD, Zhang S. Design and loss analysis of a high speed flywheel energy storage system based on axial-flux flywheel-rotor electric machines. In: 9th International Power and Energy Conference; 2010; Singapore. pp. 886-891.

[13] Lee H, Ji K, Yoo E, Park Y, Noh M.D. Design of a micro flywheel energy storage system including power converter. In: IEEE TENCON 2009 Conference; 2009; Singapore. pp. 1-6.

[14] Pena-Alzola R, Sebastian R, Quesada J, Colmenar A. Review of flywheel based energy storage systems. In: International Conference on Power Engineering, Energy and Electrical Drives; 2011; Torremolinos, Spain. pp. 1-6.

[15] Orlu U, Yuksel G, Gomes L, Hall K. BILSAT-1: Power system sizing and design. In: Proceedings of International Conference on Recent Advances in Space Technologies; 2003; İstanbul, Turkey. pp. 159-164.

[16] Schaeffler Technologies. Technical Principles: Rolling Bearings: Friction and Increases in Temperature. Herzogenaurach, Germany: Schaeffler Technologies GmbH, 2010.

[17] Pyrhönen J, Jokinen T, Hrabovcova V. Design of Rotating Electrical Machines. West Sussex, UK: John Wiley & Sons, 2008.

[18] FAG. Super Precision Bearings. Schweinfurt, Germany: Schaeffler Group Industrial, 2010.

[19] Park JD, Kalev C, Hofmann HF. Control of high-speed solid-rotor synchronous reluctance motor/generator for flywheel-based uninterruptible power supplies. IEEE T Ind Electron 2008, 55: 3038-3046.

[20] Torrey DA. Switched reluctance generators and their control. IEEE T Ind Electron 2002, 49: 3-14.

[21] Mademlis C, Kioskeridis I. Optimizing performance in current-controlled switched reluctance generators. IEEE T Energy Conver 2005, 20: 556-565.

Appendix. Motor/generator data.

Values at nominal voltage	
Nominal voltage	36 V
No load speed	64000 rpm
No load current	316 mA
Nominal speed	61600 rpm
Nominal torque (max. continuous torque)	42.2 mNm
Nominal current (max. continuous current)	8.1 A
Stall torque	1430 mNm
Starting current	266 A
Max. efficiency	93%
Characteristics	
Terminal resistance phase to phase	0.135 ohm
Terminal inductance phase to phase	0.014 mH
Torque constant	5.36 mNm/A
Speed constant	1780 rpm/V
Speed/torque gradient	44.9 rpm/mNm
Mechanical time constant	2.57 ms
Rotor inertia	5.45 gcm^2